Canadian Mineralogist
Vol. 17, pp. 619-634 (1979)

STUDIES OF THE SULFOSALTS OF COPPER
VII. CRYSTAL STRUCTURES OF THE EXSOLUTION PRODUCTS $Cu_{12.3}Sb_4S_{13}$ AND $Cu_{13.8}Sb_4S_{13}$ OF UNSUBSTITUTED SYNTHETIC TETRAHEDRITE

EMIL MAKOVICKY
Institute of Mineralogy, University of Copenhagen,
Øster Voldgade 7, DK–1350, Copenhagen K, Denmark

BRIAN J. SKINNER
Department of Geology and Geophysics, Yale University, New Haven, Conn. 06520, U.S.A.

ABSTRACT

Crystal structures of Cu-poor tetrahedrite $Cu_{\sim 12.3}Sb_4S_{13}$ and of Cu-rich tetrahedrite, $Cu_{\sim 13.8}Sb_4S_{13}$ were refined by full-matrix least-squares from counter-diffractometer X-ray data ($\theta > 30°$) obtained from their parallel-exsolved intergrowth, originally a single crystal of synthetic high-temperature phase. Respective R indices for 114 and 110 observed reflections are 4.1 and 7.4%. Both phases are cubic, isostructural with natural tetrahedrite (Wuensch 1964) in space group $I43m$, with $Z = 2$; the a values are 10.323(1) and 10.448(1) Å, respectively. The Sb–S(1) distances are 2.45 and 2.46 Å, respectively. The Cu(1) position in the Cu-poor phase has 90% occupancy, the Cu(1)–S(1) distance is 2.31 Å. That in the Cu-rich phase has 67% occupancy, with the average Cu–S distance 2.35 Å. The Cu(2) positions are fully occupied, with the Cu(2) (mean position)–S distances 2.25 (x2) and 2.25 Å, and 2.27 (x2) and 2.25 Å, respectively. If the prolate probability ellipsoids of Cu(2) are interpreted as disordered flat-pyramidal Cu(2) coordination, the Cu–S distances become 2.28–2.30 Å, and the Cu(2)–Cu(2) contacts ~ 2.76 Å. The remaining copper is mobile, with only one weak maximum (0.1 Cu) with trigonal-planar coordination located in the Cu-rich phase. The Cu-poor phase contains ~ 2 and the Cu-rich phase ~ 8 mobile Cu atoms in the cell. Both phases represent room-temperature electrolytes.

SOMMAIRE

La structure cristalline de deux "tetraédrites", $Cu_{\sim 12.3}Sb_4S_{13}$ et $Cu_{\sim 13.8}Sb_4S_{13}$, a été affinée, par la méthode des moindres carrés à matrice complète, à partir de données de diffraction X recueillies sur diffractomètre à compteur ($\theta > 30°$). Le spécimen étudié consistait en une intercroissance de démixtion des deux phases en orientations parallèles provenant d'un cristal unique d'une phase synthétique de haute température. Sur 114 et 110 réflexions observées, le résidu est, respectivement, $R = 0.041$ et $R' = 0.074$. Les deux phases, isotypes de la tetraédrite naturelle (Wuensch 1964), cristallisent en $I43m$, avec $Z = 2$ et $a = 10.323(1)$. $a' = 10.448$è1)Å comme arête de maille. Les valeurs numériques suivantes se rapportent, respectivement à la phase à faible teneur en cuivre et à la phase à forte teneur en cuivre. Distance Sb–S(1): 2.45 et 2.46 Å. Occupation de la position Cu(1): 90% et 67%. Distance Cu(1)–S(1): 2.31 et 2.35 Å. Occupation de la position Cu(2): 100% et 100%. Distances Cu(2)–S: 2.25 (x 2), 2.25 Å et 2.27 (x 2), 2.25 Å. Dans l'hypothèse où les ellipsoïdes de probabilité allongés de Cu(2) représenteraient une coordination de Cu(2) en désordre, en forme de pyramide surbaissée, on obtient, pour les distances Cu–S, 2.28-2.30 Å et, pour les contacts Cu(2)–Cu(2), ~ 2.76 Å. Le cuivre en excès est mobile, avec un seul maximum (faible, 0.1 Cu) à coordination plane trigonale, situé dans la phase la plus riche en cuivre. Le nombre d'atomes de cuivre mobiles dans la maille s'élève à ~2 et à ~ 8, respectivement. Les deux phases sont des electrolytes à la température ambiante.

(Traduit par la Rédaction)

INTRODUCTION

Tetrahedrite is the most common sulfosalt of copper in the majority of sulfide ore-deposits. Its widely accepted formula, $Cu_{12}Sb_4S_{13}$, was postulated by Pauling & Neuman (1934) in their reappraisal of Machatschki's (1928) work. Natural tetrahedrites, however, contain substantial amounts of Fe, Zn, Ag, As and Hg in solid solution, and the general formula is more nearly $(Cu,Ag)_{10}(Fe,Zn)_2(Sb,As)_4S_{13}$ (Springer 1969, Takéuchi 1970).

The Pauling & Neuman (1934) structure was refined by Wuensch (1964). Structures for Hg-rich (schwazite) and Ag-rich (freibergite) tetrahedrites were determined by Kalbskopf (1971, 1972). All these structural studies have been carried out with natural, *substituted* tetrahedrites, and the *Me*:Sb:S ratio was assumed to be 12:4:13.

With recent studies of the phase relations in the Cu–Sb–S system by Skinner *et al.* (1972) and by Tatsuka & Morimoto (1973), it is possible to determine the crystallography and composition of unsubstituted pure copper tetrahedrite. In 1965 Cambi & Elli found that tetrahedrite has a solid-solution field and observed the presence of two coexisting phases in their tetrahedrite samples. Skinner *et al.* (1972) specified the composition of the high-temperature tetrahedrite as $Cu_{12+x}Sb_{4+y}S_{13}$ ($0 \leq x \leq 1.92$; $-0.02 \leq y \leq 0.27$) and demonstrated that the two room-temperature tetrahedrite phases $Cu_{12+x}Sb_{4+y}S_{13}$ and $Cu_{14-x}Sb_{4+y}S_{13}$ represent products of a low-temperature exsolution. The room-temperature solid-solution field of tetrahedrite was also studied by Tatsuka & Morimoto (1973), but so far no one has carried out structural studies on the exsolved phases. The present paper reports our attempts to do so.

TABLE 1. CHEMICAL AND CRYSTALLOGRAPHIC INFORMATION

Estimated overall composition: $Cu_{12.59}Sb_{4.03}S_{13}$

The exsolved phases:

Cu-poor phase	Cu-rich phase
$\sim Cu_{12.3}Sb_4S_{13}$	$\sim Cu_{13.8}Sb_4S_{13}$
a = 10.323(1)A	a = 10.448(1)A
cubic, $I\bar{4}3m$	cubic, $I\bar{4}3m$

Data collection: Supper-Pace diffractometer, equi-inclination technique, rotation axis [111], CuKα radiation, step scanning, reflections with $\theta > 30^\circ$ from the two exsolved components were semi-automatically separated using reflection profiles.
Absorption correction: crystal volume $\sim 0.31 \times 10^{-4}$ cm^3 17 boundary functions, 2225 integration points inside the crystal, $\mu_1 = 750.4$ cm^{-1}.

Full matrix weighted least-squares refinement.

$R = \Sigma(||F(obs)| - |F(calc)||)/\Sigma|F(obs)|$

$R_w = (\Sigma_w(|F(obs)| - |F(calc)|)^2/\Sigma wF(obs)^2)^{1/2}$

$w = 1$ or $1/var(F(obs))$

	Cu-poor phase	Cu-rich phase
No. of F(obs)	114	110
R	4.1%	7.4%
R_w	4.1%	6.9%

Anisotropic temperature factor

$$\exp\left(-\sum_{i}^{3}\sum_{j}^{3} h_i h_j \beta_{ij}\right)$$

EXPERIMENTAL

Crystals of tetrahedrite were grown from pure Cu, Sb and S in evacuated silica glass tubes at 400°C. Only charges in the centre of the tetrahedrite composition field (Skinner *et al.* 1972) yielded single crystals of suitable quality. No suitable crystals could be grown at the limits of the elongate composition field.

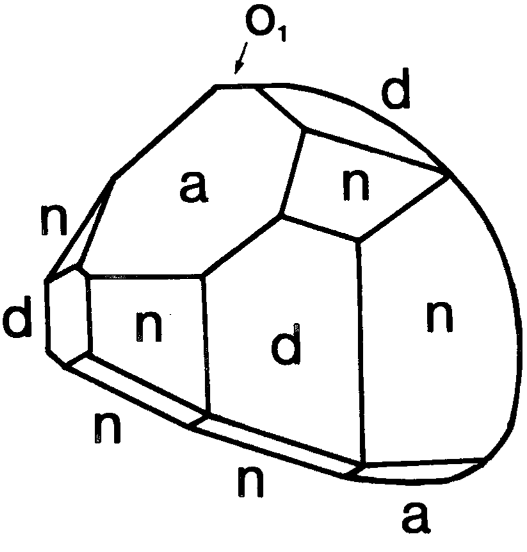

FIG. 1. Crystal faces on the studied crystal of synthetic tetrahedrite; *a* denotes {100}, *d* {110}, *n* {211} and o_1 {1$\bar{1}$1}.

Most crystals display twinning or coarse mosaic (or both) on X-ray photographs. One crystal found to be free of these phenomena was used for structure analysis. All tetrahedrites grown above 300°C undergo exsolution into Cu-rich and Cu-poor components (Makovicky & Skinner 1978). Thus, our crystal quenched to an agglomerate of rather loosely connected micrograins. Because the crystal would have disintegrated to powder if stressed, it could not be ground to a sphere in order to lessen the absorption problem. The crystal was, as far as possible, stabilized by impregnating it with synthetic resin at room temperature. The crystal used (Fig. 1) is isometric, bounded by the forms {211}, {110}, {100} and, of secondary importance, {1$\bar{1}$1}. All of them represent typical forms developed on the crystals of natural tetrahedrite (Palache *et al.* 1951).

The two tetrahedrites in the exsolved mosaic remained perfectly parallel so we had, in effect, two crystals in one. Systematic extinctions are the same, and the intensity distribution in reciprocal space is nearly the same for both phases. From the possible space groups $I\bar{4}3m$ and $I23$, the former was chosen on the basis of the structural results. The cubic lattice constants of both phases (Table 1) were refined from the quartz-calibrated Weissenberg photographs using 22 reflections for each phase and extrapolating the calculated *a* values to $\theta = 90°$ by the Nelson & Riley (1945) formula.

Intensity data were collected on an automated Supper-Pace single-crystal diffractometer in the laboratory of Dr. L. Finger, Carnegie Institution, Washington, D.C. Equi-inclination strategy (ω-scan) and monochromatic Cu $K\bar{\alpha}$ radiation were used. The entire region of each pair of reflections with the same *hkl* indices was step-scanned. Step increments were 0.05°, step counting was times 3 seconds, and number of steps *per* reflection pair was from ~ 50 to ~ 300. The rotation axis was [111] for both components. X-ray intensities of the two exsolved phases were collected in two separate runs, each at its appropriate diffraction angles.

Owing to the almost complete overlap of the reflections of the two phases at low diffraction angles, only the reflections with θ angles above 30° were subjected to the peak-separation procedures. Each measurement peak was separated from the accompanying peak of the other phase by a series of semi-automatic procedures. The entire range of every peak scan was plotted out in a computer output of suitable format (Fig. 2). The principal points describing peak widths and peak maxima were located from it. The principal points were then used for computer separation of the two peaks, the results again checked and, if necessary, reprocessed using the modified plots. The only assumption used in the programs was that peak profiles were symmetrical. The assumption was confirmed for all well-defined peaks, and it is a logical consequence of the ω-scan strategy from a half-spherical crystal mounted with the flat basis nearly perpendicular to the rotation axis. Standard errors for the final intensities were obtained from the counting statistics, and were augmented appropriately when only a part ($\geqq$ one half) of the examined peak could be separated from the overlap with the interfering peak. Scan plots allowed us to assess intensities for all weakest to zero-intensity reflections. At the high diffraction angles, where the reflections become split into their α_1 and α_2 components (*i.e.*, they become asymmetrical), the angular difference of the corresponding reflections of the two exsolved tetrahedrites is such that their peaks are completely separated.

All measured reflections were subjected to the absorption and Lorentz–polarization corrections. Absorption corrections were carried out using the program written by C. T. Prewitt after Wuensch & Prewitt (1965).

The mounted crystal was microphotographed in 30 different orientations. By combining photographs, distances between crystal faces and the crystal centre could be accurately estimated for all 15 crystal faces (Fig. 1). The remaining surface was closely described by an ellipsoid slightly elongate along the rotation axis [111], and the growth base was approximated by the closest fitting crystal face, (111). The linear absorption coefficient for the average composi-

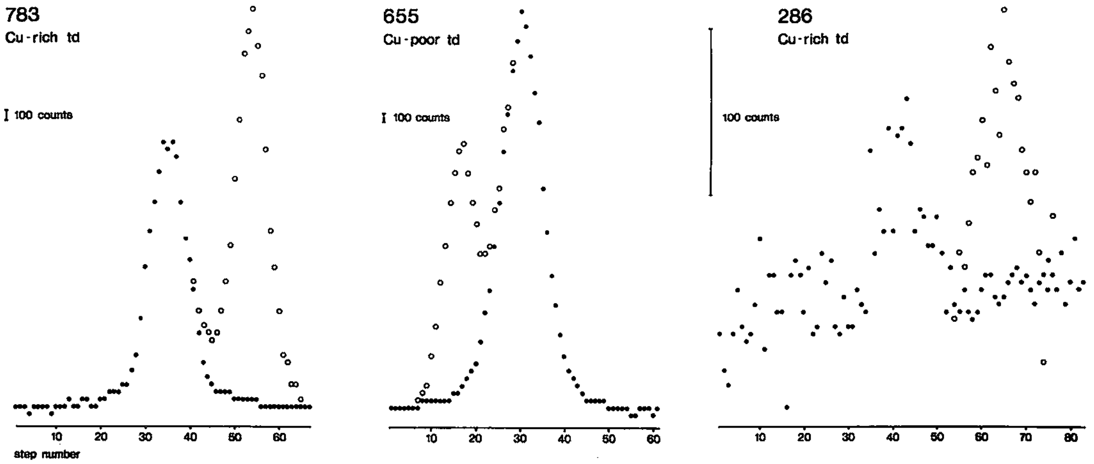

FIG. 2. Simulated plots of selected step-scanned X-ray reflections of the studied crystal which contains two parallel, exsolved tetrahedrite end-members. Full circles denote net step-count values after peak separation, empty circles denote the peak of the other end-member (with the same *hkl* indices), subtracted during the separation. 783 and 655 are strong reflections, 286 a very weak reflection.

tion of the composite crystal and Cu $K\bar{\alpha}$ radiation is high, 750.4 (95% of the original value to account for the void cracks). If we had used Mo radiation to reduce absorption, we would have greatly diminished the shell of paired reflections sufficiently split to allow reliable separation of individual peaks. A nonlinear grid of 20x20x20 integration points, their density increasing towards the crystal surface, was used for absorption correction. Altogether there were 2225 integration points inside the crystal as defined by the above 16 planar and 1 ellipsoidal boundary functions. The total volume of the crystal was estimated to be ~ 0.31×10^{-4} cm^3. It can be approximately circumscribed by a sphere with a radius of 0.025 cm. Transmission factors for individual reflections varied between 0.020 and 0.003. No extinction correction was performed because of the pronounced mosaic character of the crystal with cracks and ensuing block misorientation.

Equivalent corrected structure-factors were weighted and averaged, with the weights indirectly proportional to the structure-factor variances obtained from counting statistics, to which both the Lorentz–polarization and the absorption corrections had been applied. The larger of the two resulting variances of the mean, the external or the internal (Deming 1964), represents the accuracy of the final structure-factors and was used in the weighted least-squares refinements. The overall $\sigma(F)/F$ ratio for the strong and medium reflections is 0.036. Step-scanning enabled us to obtain directly the F_{obs} and $\sigma(F)$ values even for the weakest reflections so that no minimal $F/\sigma(F)$ cutoff value was introduced. Two to four equivalent reflections were averaged in each case, the average being 2.4 measurements for each independent reflection. The reflections with $h, k, l > 0$ were used in further refinement; the remaining reflections were employed in the attempts to establish the absolute configuration of the two tetrahedrite structures. After each step in data reduction, the reflections were examined and those showing the consequences of bad peak-separation were excluded. The last check was based on difference-Fourier maps where reflections causing false ripples without symmetry equivalents were sought and three of them eliminated. The structure analysis of the

TABLE 2. INDEPENDENT POSITIONAL AND THERMAL PARAMETERS FOR THE CRYSTAL STRUCTURES OF TETRAHEDRITES

Atom	Equipoint	Atomic parameters	$Cu_{12.3}Sb_4S_{13}$ present work	$Cu_{13.8}Sb_4S_{13}$ present work	$Cu_{10.4}Zn_{1.2}Fe_{0.3}Sb_4S_{13}$ Wuensch (1964)
Cu(1)	$\frac{1}{4}\frac{1}{2}0$	site occupancy	0.90(1)	0.67(2)	1.00 fixed
	12d	β_{11}	0.0072(4)	0.0057(7)	0.0028(3)
		β_{33}	0.0055(2)	0.0044(3)	0.0027(2)
Cu(2)	x00	site occupancy	1.01(2)	0.99(3)	1.00 fixed
	12 e	x	0.2180(5)	0.2157(8)	0.2150(5)
		β_{11}	0.0062(4)	0.0044(5)	0.0032(5)
		β_{22}	0.0192(4)	0.0201(5)	0.0130(6)
		β_{23}	-0.0118(5)	-0.0142(7)	-0.0094(14)
S(1)	xxz	site occupancy	0.99(1)	0.99(2)	1.00 fixed
	24 g	x	0.1144(2)	0.1137(5)	0.1152(3)
		z	0.3635(4)	0.3613(7)	0.3609(5)
		β_{11}	0.0037(1)	0.0040(2)	0.0030(3)
		β_{33}	0.0031(5)	0.0035(5)	0.0026(4)
		β_{12}	-0.0004(3)	-0.0013(5)	-0.0008(4)
		β_{31}	0.0002(2)	-0.0006(3)	-0.0001(3)
S(2)	000	site occupancy	0.89(5)	1.04(9)	1.00 fixed
	2 a	β_{11}	0.0049(7)	0.0049(9)	0.0027(6)
Sb	xxx	site occupancy	1.00 fixed	1.00 fixed	1.00 fixed
	8 c	x	0.2683(1)	0.2663(2)	0.2682(1)
		β_{11}	0.0032(1)	0.0050(1)	0.0026(1)
		β_{12}	-0.0003(1)	-0.0011(1)	-0.0003(1)

The numbers in parentheses represent calculated standard errors and refer to the last decimal place

TABLE 3. RESULTS OF THE PRINCIPAL REFINEMENT STAGES FOR SYNTHETIC TETRAHEDRITES

Phase:		$Cu_{12.3}Sb_4S_{13}$						$Cu_{13.8}Sb_4S_{13}$				
Temp. factors:		B	B	$\underline{\beta}$	$\underline{\beta}$	$\underline{\beta}$	$\underline{\beta}$	B	B	$\underline{\beta}$	$\underline{\beta}$	$\underline{\beta}$
Refinement type:		init.			rad.	enant.	cons.	init.				enant.
F(obs) weights:		1	1	1	1/var	1/var	1/var	1	1	1	1/var	1/var
Atom	Parameter						final				final	
Cu(1)	site occup.	1.0**	1.0**	0.94	0.89	0.88	0.90	1.0**	0.66	0.66	0.67	0.66
	B*(A²)	1.19	2.29	2.33	2.64	2.56	2.59	1.19	2.06	1.98	2.11	2.03
	x⁺	1/4	1/4	1/4	1/4	-1/4	1/4	1/4	1/4	1/4	1/4	-1/4
	y⁺	1/2	1/2	1/2	1/2	-1/2	1/2	1/2	1/2	1/2	1/2	-1/2
	z⁺	0	0	0	0	0	0	0	0	0	0	0
Cu(2)	site occup.	1.0**	1.00**	0.99	1.01	1.04	1.01	1.0**	0.96	0.95	0.99	0.98
	B*(A²)	4.19	4.77	6.20	6.49	6.79	6.34	4.19	5.38	6.33	6.49	6.35
	x	.2150	.2098	.2129	.2186	-.2188	.2180	.2150	.2141	.2151	.2157	-.2159
	y⁺ = z⁺	0	0	0	0	0	0	0	0	0	0	0
S(1)	site occup.	1.0**	1.0**	1.02	0.98	0.99	0.99	1.0**	1.00	1.00	0.99	1.00
	B*(A²)	1.23	1.26	1.41	1.46	1.46	1.49	1.23	1.69	1.51	1.67	1.67
	x = y	.1152	.1132	.1141	.1145	-.1145	.1144	.1152	.1146	.1146	.1137	-.1140
	z	.3609	.3625	.3625	.3635	-.3636	.3635	.3609	.3611	.3616	.3613	-.3612
S(2)	site occup.	1.0**	1.00**	1.10	0.89	0.87	0.89	1.0**	1.03	1.08	1.04	1.00
	B*(A²)	1.14	2.18	2.38	1.96	1.77	2.09	1.14	1.95	1.96	2.14	2.17
	x⁺ = y⁺ = z⁺	0	0	0	0	0	0	0	0	0	0	0
Sb	site occup.	1.0**	1.0**	1.0**	1.0**	1.0**	1.0**	1.0**	1.0**	1.0**	1.0**	1.0**
	B*(A²)	1.11	1.27	1.32	1.37	1.34	1.38	1.11	1.98	2.10	2.18	2.16
	x = y = z	.2682	.2687	.2683	.2683	-.2683	.2683	.2682	.2668	.2664	.2663	-.2662
Bond lengths (A)												
Cu(1) - S(1)			2.321	2.317	2.311	2.310	2.311		2.376	2.350	2.353	2.354
Cu(2) - S(1)			2.284	2.272	2.242	2.243	2.246		2.288	2.283	2.267	2.268
Cu(2) - S(2)			2.165	2.197	2.257	2.258	2.250		2.237	2.247	2.254	2.256
Sb - S(1)			2.468	2.453	2.451	2.451	2.452		2.455	2.454	2.462	2.458
R		13.1	11.1	7.3	4.1	4.1	4.1	21.4	14.9	9.2	7.7***	9.0
R_w		16.6	10.8	7.7	4.1	4.3	4.1	20.7	14.9	9.7	7.1***	9.2

* isotropic temperature factor or 'equivalent isotropic temperature factor' after Hamilton (1959)

** parameters kept fixed during the refinement

*** R drops to 7.4/6.9% with Cu(3) (site occupancy ≈ 0.10, equivalent B≈9.17, x=y≈0.290 and z≈0.030) included in the final refinement

⁺ parameters with values determined by symmetry

Abbreviations: B - individual isotropic temperature factors, $\underline{\beta}$ - anisotropic temperature factors; init. - initial values (Wuensch 1964); rad./cons./enant. - radical/conservative/enantiomorph refinement; var - variance of F(obs).

Cu-poor tetrahedrite was based on the total of 114 nonequivalent reflections, that of the Cu-rich tetrahedrite on 110 reflections.

STRUCTURE DETERMINATION AND REFINEMENT

The parameter values obtained by Wuensch (1964) on natural tetrahedrite (Table 3) served as the starting set for both tetrahedrites. However, the set was not applied uncritically. Three-dimensional Patterson functions of both phases were compared with a calculated Patterson function of Wuensch's tetrahedrite. Fourier functions were also calculated for both, using the phases obtained only on Sb (and then on Sb and S1) atoms, in order to verify the Cu positions. All three-dimensional Fourier syntheses were performed with Ahmed's (1968) program NRC–8. The difference Fourier based on the *F*(calc.) values calculated from Wuensch's tetrahedrite and the *F*(obs.) values of the Cu-rich phase showed immediately that the Cu(1) position was partly vacant.

Both structures were refined by means of the full-matrix least-squares program ORFLS (Busing *et al.* 1962) modified by E. Makovicky to include anomalous dispersion corrections. Scattering curves for neutral Cu, Sb and S after Cromer & Waber (1965) were used together with anomalous dispersion coefficients for these elements by Cromer (1965). In the first stage of the refinement, unit weights and isotropic individual temperature-factors were employed (Table 3). In this stage of refinement all positional parameters not constrained by symmetry, all individual temperature factors and, in the case of the Cu-rich phase, the site occupancies were refined. Only the occupancy of the Sb position was kept fixed at 1.0 in either phase, in agreement with the composition of the sample in the phase diagram. This assumption was confirmed by the resulting site-occupancies of S(1), Cu(2) and partly also S(2). All of them were within refinement accuracy equal to unity. The occupancy of Cu(1) in the Cu-rich phase was refined from 1.0 to 0.67 with a considerable gain in the *R* value (Table 3). It did not depart from 0.67 in any of the consecutive refinement stages.

After the parameter shifts became insignificant with respect to the relevant standard errors ($\Delta p \leqq 1/3\ \sigma_p$), anisotropic temperature-factors were introduced. For both phases a major decrease in the *R* values was observed when the pronounced anisotropy of the "thermal ellipsoid" of Cu(2) was considered (Table 3). The observation weights were introduced after the completion of this refinement stage. Again, the structures were refined until the parameter shifts became insignificant when compared with standard errors (Tables 2 and 3).

A single scale-factor was used for all reflections of each phase through most refinement stages. In the last stage, three scale-factors related to the ζ coordinates of reflections during the collection of intensities were used.

The refinement attempts in the space group *I*23 did not give results significantly different from those in the space group $I\bar{4}3m$. The latter was accepted as final for both structures.

For both phases enantiomorphous orientations were extensively refined. However, the differences between the structure parameters obtained for the two orientations lay mostly within the limits of the estimated standard errors. Thus, the absolute orientation could not be established. These results are similar to those of Wuensch *et al.* (1966); we follow them in preferring the orientation with the better agreement factor (Tables 2 and 3).

The highly regular character of the crystal structure of tetrahedrite brings about fairly strong interactions between some structure parameters during the refinement. The strongest interactions occur between the parameters of Cu(1) and of Cu(2). The highest positive correlation-coefficients tie β_{11} of Cu(1) with *x* of Cu(2) and β_{12} of Cu(2) with β_{22} of the same atom.

Therefore, both the radical and the conservative approaches were tried in full for the Cu-poor phase. In the first approach, with fast convergence, the parameters were refined simultaneously even if they displayed a high degree of correlation. In the second approach, the simultaneous refinement of highly correlated parameters was largely avoided, and the convergence was slowed down by the use of suitable damping factors for parameter shifts (Sparks 1961). The results of the two approaches can be compared in Table 3. The only important differences are those in the positional parameter *x* of Cu(2). This parameter, which significantly influences the experimental values for the Cu(2)–S bond lengths, suffers most from correlation problems during the refinement and has the largest standard errors of all positional parameters (Table 2; *cf.*, Table 2 in Wuensch *et al.* 1966).

From the start of the structure determinations we were aware of the apparent absence of a large part of the copper indicated by the composition of the Cu-rich phase. In each stage of determination and refinement, attempts were made to locate the missing copper atoms. Numerous spurious maxima in the Fourier maps were tried out. In later stages, all imaginable positions for the additional and substitutional copper atoms in the more-or-less refined structure of the Cu-rich phase were tried, with varying site-occupancies and temperature-factors. None of the positions was found to be occupied: there is no additional Cu in or around the [Cu(1)S_4] tetrahedra, close to the [Cu(2) S_3] triangles, nor replacing a part of the [SbS_3] coordination pyramids. Nor is there additional copper in the empty tetrahedra in the structure or in the void space of the Cu(2) spinners of Wuensch (1964). Once the structure refinement of the Cu-rich phase was completed with the basic set of atoms given in Table 2, the difference-Fourier map showed small but well-defined maxima of what was subsequently refined as the partly occupied Cu(3) position (Table 3). No additional indications of copper were found in the final Fourier and difference-Fourier maps of both exsolved tetrahedrite phases. No spurious maxima were found in the difference maps, located on or around the refined copper and sulfur atoms [including Cu(2)], indicating their good positional refinement. No electron-density bridges connecting Cu(1) with Cu(2) and Cu(2) with Cu(2)′ were observed.

DESCRIPTION AND DISCUSSION OF THE STRUCTURES

The final atomic parameters are given in

Table 2 together with the parameters determined by Wuensch (1964) for the natural tetrahedrite of approximate composition $Cu_{10.4}Zn_{1.2}Fe_{0.3}Sb_4S_{13}$. The root-mean-square displacements of the atoms along the principal axes of the vibration (or disorder) ellipsoids, together with the orientation of the ellipsoids, are given in Table 5. Principal interatomic distances and angles are given in Table 4, again compared with the corresponding data of Wuensch (1964). Representative fragments of the two structures, drawn by ORTEP (Johnson 1965), are shown in Figures 3 and 4. Observed and calculated structure factors (Table 6) have been deposited and may be obtained at nominal charge from the Depository of Unpublished Data, CISTI, National Research Council of Canada, Ottawa, Ontario K1A 0S2.

The crystal structures of both the Cu-poor and the Cu-rich unsubstituted tetrahedrite conform to the principles established for tetrahedrite by Pauling & Neuman (1934) and by Wuensch (1964).

The [SbS_3] pyramids

The sturdiest element in the structure, least influenced by the formation of interstitial and substitutional solid solutions (Cu^I, Cu^{II}, Zn, Fe), is the [SbS_3] pyramid. The Sb–S(1) interatomic distances show slight compression and distension in the Cu-poor and Cu-rich phase,

TABLE 4. SELECTED INTERATOMIC DISTANCES AND ANGLES FOR TETRAHEDRITES

Bond or distance	$Cu_{12.3}Sb_4S_{13}$ present work	$Cu_{13.8}Sb_4S_{13}$ present work	$Cu_{10.4}Zn_{1.2}Fe_{0.3}Sb_4S_{13}$ Wuensch (1964)
Cu(1)-S(1)	2.311(4)A	2.353(7)A	2.342(4)A
Cu(2)-S(1)	2.246(7)	2.267(11)	2.272(10)
Cu(2)-S(2)	2.250(6)	2.254(9)	2.234(5)
Sb-S(1) in the SbS_3 pyramid	2.452(4)	2.462(7)	2.446(7)
Sb-S(1)	4.010(4)	4.065(7)	4.033(5)
S(1)-S(2)	4.107(3)	4.132(6)	4.114(5)
S(1)-S(1) in the Cu(2)S_3 co-ordination triangle	3.341(5)	3.361(9)	3.386(5)
Cu(2)-Cu(2) not corrected for thermal motion	3.186(8)	3.188(12)	3.159(8)
Cu(1)-Cu(2)	3.889(7)	3.955(9)	3.939(7)
S(1)-S(1) in the SbS_3 co-ordination pyramid	3.636(6)	3.658(10)	3.611(6)
S(1)-S(1) the edge perpendicular to $\bar{4}$ of the Cu(1)S_4 tetrahedron	3.678(5)	3.748(9)	3.753(5)
S(1)-S(1) the diagonal edge of the Cu(1)S_4 tetrahedron	3.821(6)	3.900(10)	3.859(6)
Bond angles			
S(1)-Sb-S(1)	95.70(10)°	95.92(20)°	95.13(25)°
S(1)-Cu(2)-S(1)	96.04(25)	95.72(40)	96.31(30)
S(1)-Cu(2)-S(2)	131.98(10)	132.14(20)	131.85(15)
S(1)-Cu(1)-S(1) edge normal to $\bar{4}$	105.45(15)	105.58(25)	106.50(20)
S(1)-Cu(1)-S(1) diagonal edge	111.52(15)	111.94(25)	110.97(15)

Estimated standard errors (in parentheses) refer to the last decimal place.

TABLE 5. MAGNITUDES AND ORIENTATIONS OF THE PRINCIPAL AXES OF THE THERMAL ELLIPSOIDS FOR THE STRUCTURES OF SYNTHETIC TETRAHEDRITES

		$Cu_{12.3}Sb_4S_{13}$				$Cu_{13.8}Sb_4S_{13}$			
Atom	Ellipsoid axis	r.m.s. displacement	Angles to crystal axes			r.m.s. displacement	Angles to crystal axes		
			a_1	a_2	a_3		a_1	a_2	a_3
Cu(1)	1	0.172Å	90°	90°	0°	0.155Å	90°	90°	0°
	2	0.172	90	90	180	0.155	90	90	180
	3	0.200	0	90	90	0.177	0	90	90
Cu(2)	1	0.184	0	90	90	0.155	0	90	90
	2	0.198	90	135	135	0.179	90	135	135
	3	0.410	90	135	45	0.436	90	135	45
S(1)	1	0.124	116	116	38	0.111	54	54	57
	2	0.138	124	124	128	0.148	67	67	147
	3	0.149	45	135	90	0.172	45	135	90
S(2)	1	0.163	-			0.165	-		
	2	0.163	-			0.165	-		
	3	0.163	-			0.165	-		
Sb	1	0.121	55	55	55	0.123	55	55	55
	2	0.138	66	66	145	0.183	66	66	145
	3	0.138	114	114	35	0.183	114	114	35
'Cu(3)'	1					0.22	55	55	55
	2					0.39	114	114	36
	3					0.39	114	114	35

respectively, compared to the Sb–S(1) distances in $Cu_{10.4}Zn_{1.2}Fe_{0.3}Sb_4S_{13}$ (Wuensch 1964). However, they are longer than the corresponding distances in freibergite (Kalbskopf 1972), in which the $[SbS_3]$ pyramids are compressed between the expanded, triangular arms $[(Cu, Ag)(2)S_3]$ of the spinners (Wuensch 1964, Fig. 5). The S(1)–S(1) distances and the S(1)–Sb–S(1) angles in the $[SbS_3]$ pyramids of the phases studied are slightly larger than in the substituted tetrahedrite (Wuensch 1964). The observed Sb–S(1) distances are in good agreement with the average Sb–S distances in the sulfosalts with isolated $[SbS_3]$ groups (Kupčík 1974, Table 51-A-2).

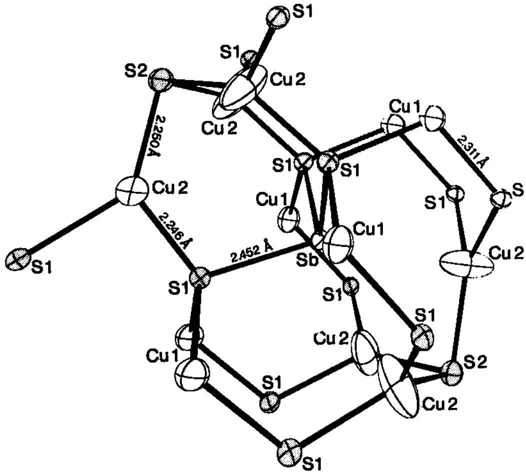

FIG. 3. Fragment of the crystal structure of Cu-poor tetrahedrite between (0,0,0) (upper left-hand corner) and $(\overline{\tfrac{1}{2}}, \tfrac{1}{2}, \overline{\tfrac{1}{2}})$ (lower right-hand corner). Unit-cell edges are parallel to the S(2)–Cu(2) bonds at (0,0,0). ORTEP drawing with 50% probability ellipsoids. Sulfur atoms are shaded.

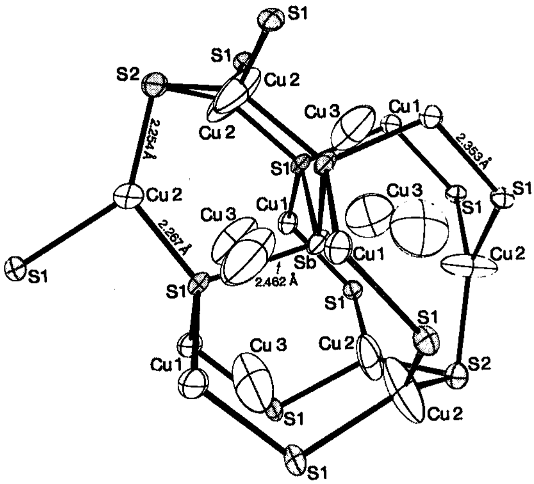

FIG. 4. Fragment of the crystal structure of Cu-rich tetrahedrite. The description, size and orientation of the fragment are the same as in Figure 3. ORTEP drawing.

The $[Cu(1)S_4]$ tetrahedra

The $[Cu(1)S(1)_4]$ tetrahedra are only partly occupied by stationary Cu in both structures (Table 2). In both cases Cu(1) displays essentially isotropic and moderate thermal motion. The increase of the Cu(1)–S(1) distances by 0.04 Å (~ 2 rel. %) between the minimal and the maximal Cu contents in the tetrahedrites studied represents the most spectacular change in the stationary skeleton of unsubstituted tetrahedrites. If we linearly extrapolate the dependence of the Cu(1)–S(1) distance on the occupancy of the Cu(1) position, this distance in the fully occupied tetrahedron would represent 2.295(5) Å. It is close to the tetrahedral Cu–S distances in chalcopyrite (2.302 Å: Hall & Stewart 1973), cubanite (av. 2.305 Å: Szymanski 1974), Cu(1) in luzonite (2.304 Å: Marumo & Nowacki 1967), and in lautite (2.289 and 2.304 Å: Marumo & Nowacki 1964).

The partial occupancy of the Cu(1) position shows that in the Cu-rich phase one out of three tetrahedra is void with respect to stationary copper. Extrapolating the above linear plot towards zero occupancy for Cu(1), we obtain the tetrahedron centre–S(1) distance of 2.47(2) Å. The triangular faces of a void tetrahedron will have the centre-to-corner distances of ~ 2.33 Å and will allow free passage of Cu ions, similar to the triangular coordinations in high skinnerite at 170°C (2.254, 2.282 and 2.284 Å: Makovicky & Skinner, unpubl. data), and to the faces of tetrahedra in high chalcocite (2.25 and 2.33 Å (3x) after Buerger & Wuensch 1963, 2.287 and 2.329 Å (3x) after Sadanaga *et al.* 1965).

Naturally, the vacant $[CuS_4]$ tetrahedra are not entirely vacant with respect to mobile copper atoms, and their dimensions should be somewhat smaller than the extreme dimensions calculated for them above. The triangular faces of the average, two-thirds occupied (*i.e.*, non-extrapolated) tetrahedra have the centre-to-corner distances of only ~ 2.22 Å, below the average Cu–S distances of stationary triangular planar copper coordination (Table 7).

In both phases studied the $[Cu(1)S_4]$ tetrahedron is distended along the $\bar{4}$ axis. The elongation is more pronounced, in both cases, than in the substituted tetrahedrite (Wuensch 1964) and can be seen from the S(1)–Cu(1)–S(1) angles and S(1)–S(1) edges given in Table 4. Orientational calculations on tetrahedrite models with fixed spinners and varying Cu(1)–S distances (Makovicky, in prep.) show that only a small part of distension can be derived from the structural adjustments connected with decreasing Cu(1)–S distances. Consequently, the principal reason for the more regular character of the [(Cu, Zn, Fe) (1)S_4] tetrahedron in the substituted tetrahedrite studied by Wuensch (1964) is its partial occupation by Zn and Fe, both of which require regular tetrahedral coordination (*e.g.*, Hall & Stewart 1973).

Tetrahedra of Cu with higher site-symmetries in well-refined structures are typically distorted (usually flattened, perhaps for accommodational reasons), with S–Cu–S angles grouped around ~ 108.5° and ~ 111°, respectively (tennantite: Wuensch *et al.* 1966; chalcopyrite: Hall & Stewart 1973; luzonite: Marumo & Nowacki 1967; covellite: Kalbskopf *et al.* 1975, Evans & Konnert 1976).

The [Cu(2)S_3] triangles

Cu(2) occurs in trigonal planar coordination similar to that described by Wuensch (1964), as an octahedral group of six copper atoms (6[CuS_3] triangles), centred on S(2) and enclosed in a cage of tetrahedra (Belov & Pobedimskaya 1969). Our results suggest that Cu(2) is more centrally positioned in the [Cu(2)S(2) S(1)$_2$] triangle than indicated by Wuensch (1964), with the Cu(2)–S(2) distance of 2.25 Å instead of 2.23 Å. Because of strong correlations, the x parameter of Cu(2) represents the least accurate of all positional parameters (Tables 1 and 4; *cf.*, Table 2 in Wuensch 1964). Table 3 shows its systematic increase as the refinement proceeded towards its final form (weighted anisotropic refinement), together with the corresponding changes in the Cu(2)–S distances. It shows that the x parameter is sensitive to the conditions of the refinement and that caution should be exercised when comparing results of different refinements.

Table 4 shows that all interatomic distances in the Cu(2) spinners of the Cu-poor phase are shorter than those in the Cu-rich (or substituted) phase. However, if the S(1)–S(2) distance is taken as a measure of spinner compression (Table 4), we see that the spinners of Wuensch (1964) and of our Cu-poor tetrahedrite have about the same radii, whereas the radius of the spinner in the Cu-rich phase is significantly larger. Thus, the reduction in the Cu(2)–S distances and in the Sb–S van der Waals contact distances (Wuensch 1964) in the Cu-poor phase stems from the reduced S(1)–S(1) distance in the narrower [Cu(2)S_3] coordination triangles (Table 1) rather than from the reduction in the radius of the spinner cavity. The cavity in the Cu-rich phase is expanded, but the reduced S(1)–S(1) distances in the [Cu(2)S_3] triangles and the expansion of the [SbS_3] pyramid make the corresponding increase in the intercavital *Me*–S distances less appreciable.

The Cu(2)–S distances

Similarly to substituted tetrahedrite (Wuensch 1964) and tennantite (Wuensch *et al.* 1966), Cu(2) in both unsubstituted tetrahedrites displays markedly anisotropic "thermal" motion. Root-mean-square displacement in the direction perpendicular to the planes of the [Cu(2)S_3] coordination triangles is 2 to 2.5 times larger than in the planes (Table 5). This "thermal motion" is not accompanied by a corresponding displacement of the sulfur atoms attached to Cu(2). If only the displacement of Cu(2) is taken into account by placing the Cu(2) atoms at the r.m.s. distance from their mean positions, the Cu(2)–S distances will be as follows: 2.287 and 2.283 Å (2x) in the Cu-poor phase, 2.296 and 2.308 Å (2x) in the Cu-rich phase, and 2.261 and 2.299 Å (2x) in Wuensch's (1964) tetrahedrite. These distances (respective averages are 2.284, 2.304 and 2.286 Å) correspond well to the observed Cu–S distances for the triangular copper coordination in sulfides and sulfosalts (Table 7). The only exceptions are the triangular nets with a tight [Cu(1)S_3] coordination in covellite (Kalbskopf *et al.* 1975, Evans & Konnert 1976), which even at r.m.s. distances display short Cu–S bonds (Table 7).

Further refinement was attempted using the split Cu(2) position, similar to the procedure tried by Kalbskopf (1972) on freibergite and by the above authors on covellite. As in these cases, the results did not differ significantly from those using the single Cu position (x,0,0).

The Cu(2)–Cu(2) distances

Displacement of Cu(2) from the mean positions alters significantly the Cu(2)–Cu(2) distances from those given in Table 4. The six Cu(2) atoms will be statistically distributed over 12 flat-pyramidal sites lining the four voids in the spinner cavity (Wuensch 1964, Fig. 5). Unavoidably, at least some of them will define short Cu–Cu contacts. For the calculated r.m.s. displacement it follows that the two (or three)

TABLE 7. Cu-S AND Cu-Cu DISTANCES IN SELECTED SULFIDES, SULFOSALTS AND CHELATES WITH S LIGANDS

Compound (mineral)	Source	Cu-S distances (in Å) in triangular $[CuS_3]$ co-ordination		Short Cu-Cu distance (in Å) triangular and/or tetrahedral Cu	
		range of all individual distances	averages for individual triangles	distance (note)	$[Cu_n]$group
tetragonal $Cu_{1.96}S$	Janosi (1964) (also SR <u>29</u>/1964)	2.31	2.31	2.71,2.96(2x), 2.97(4x)	
anilite Cu_7S_5	Koto & Morimoto (1970)	2.241-2.352	2.279, 2.313, 2.302	2.636-2.960 (range) (2.797-2.840 primarily)	network
low chalcocite Cu_2S	Evans (written comm., 1975)	typical averages over 21 co-ordination triangles	2.29-2.33	no quantitative data published	
covellite CuS	Evans & Konnert (1976)	2.191 2.200	←Cu1 "at rest"→ ←Cu1 at r.m.s. dev.→	3.199 3.055	Cu1-Cu2, network
covellite CuS	Kalbskopf et al. (1975)	2.195 2.209	←Cu1 "at rest"→ ←Cu1 at r.m.s. dev.→	3.204 3.027	Cu1-Cu2, network
stromersyite CuAgS	Frueh (1955)	2.26-2.29	2.28	-	-
α-$BaCu_4S_3$	Iglesias et al. (1972)	2.282-2.437	2.302 2.334	2.754-2.965 2.573-2.850	4 bonds 4 bonds
		deformed tetrahedral Cu*		2.573-2.850 2.677	4 bonds 2 bonds network
β-$BaCu_4S_3$ (>640°C)	Iglesias et al. (1972)	2.284-2.337	2.302	2.690	2 bonds
		deformed tetrahedral Cu*		2.557-2.690	4 bonds network
$RbCu_4S_3$	Rüdorff et al.(1952)	tetrahedral Cu		2.78(4x) 2.98	network
KCu_4S_3	Rüdorff et al.(1952)	tetrahedral Cu		2.76(4x) 2.93	network
Mooihoekite $Cu_9Fe_9S_{16}$	Hall & Rowland (1973)	tetrahedral Cu & Fe		2.73 2.69	metal clusters, presumably Fe-Cu bonds
low bornite Cu_5FeS_4	Koto & Morimoto (1975)	-		2.755 (the shortest distance)	pairs
wittichenite Cu_3BiS_3	Kocman & Nuffield (1973)	2.255-2.348	2.292,2.274 2.289	2.610,2.743, 2.944	chain also Matzat (1972)
$Bi_2Cu_3S_4Cl$	Lewis & Kupčík (1974)	2.29-2.49	2.37	2.87,2.79, 2.91 (the shortest distances)	(chains)
$Cu_4Bi_5S_{10}$	Mariolacos et al. (1975)	2.258, 2.316(2x)	2.300	-	-
cuprobismutite $Cu_{2.58}Bi_{3.14}S_6$	Ozawa & Nowacki (1975)	2.246-2.338	2.307 Cu1, full occup.	2.79-2.95	pairs Cu substituting for Bi
$Cu_4Bi_4S_9$	Takéuchi & Ozawa (1975)	2.23-2.34	2.25,2.31	2.71	chains
hodrushite $Cu_8(Bi,etc.)_{12}S_{22}$	Kupčík & Makovicky (1968)	2.26-2.35	2.31,2.32, 2.31	- -	
$(Pb_{1-x},Bi_x)Bi_2Cu_2Cu_{2-x}S_5I_2$ (x=.88)	Ohmasa & Mariolacos (1974)	2.267 2.285(2x)	2.280 (flat pyramidal, elevation =0.4Å)	2.781, 3.020	zig-zag chains
$(Cu_8L_6)(As\text{Ø}_4)_4$ $L=\left[\begin{smallmatrix}-S\\-S\end{smallmatrix}{>}C-C{<}\begin{smallmatrix}CN\\CN\end{smallmatrix}\right]^{2-}$	McCandlish et al. (1968)	2.237-2.266	2.245,2.246 2.262,2.251	2.783-2.871 mean 2.828	cubic group $[Cu_8]$ Cu's triangularly co-ordinated by S
$[(C_3H_7)_2NCOSCu]_6$	Hesse & Aava (1970)	-	-	2.701-3.057 mean 2.882	octahedral group $[Cu_6]$. Cu's flat pyramidal bound to 2 S + 10
$Cu_4[(i\text{-}C_3H_7O)_2PS_2]_4$	Lawton et al. (1972)	2.247-2.289	2.272,2.269 2.263,2.264	2.706-2.775, 2.945-2.954	tetrahedral group of $[Cu_4]$ Cu's triangularly bound to S

copper(2) atoms which are displaced towards each other from the places of their coordination triangles will lie as close as 2.77, 2.75 and 2.81 Å from each other, respectively, in the Cu-poor, Cu-rich and the substituted tetrahedrite (Wuensch 1964).

Recent structure refinements have yielded many examples of pairs, groups or networks of Cu atoms with short Cu–Cu contacts of the order of 2.6–2.9 Å, both in tetrahedral and trigonal–planar coordinations with sulfur (Table 7, also Wells 1975). The metal–metal distances are generally longer than the Cu–Cu distance in metallic copper (2.56 Å, Donnay & Ondik 1973), indicating correspondingly weaker interactions. Their spread is large. Together with the magnitude of the shortest Cu–Cu interactions, the spread primarily represents a function of the steric properties of the given (covalent) structure type, rather than of the Cu–S distances or of the size of cations involved in the structure. From a literature review by E. Makovicky it is apparent that reliable structural data (SB and SR) on the hydride, nitride, phosphides, arsenides, silicide and tellurides of Cu demonstrate the same situation, together with the insensitivity of minimal Cu–Cu distances to the size of the anion involved. Only in some metallo-organic structures the small sizes of bonding O, C, N (or P) seem to allow, where the attached ligands permit, short Cu–Cu contacts of 2.42–2.45 Å. In simpler Cu_mX_n structures the minimal Cu–Cu distances start between 2.55 and 2.70 Å; in complicated structures (usually with additional cations) they may start above 2.40 Å, or only above 2.70 Å]. The Cu–S and Cu–Cu distances in chelates with bonding sulfur atoms are comparable with those in sulfides (Table 7). Some of the typical aggregates of copper atoms in sulfides, *i.e.*, pairs, quintets, infinite chains, layers, tetrahedral, octahedral and cubic groups, $[Cu_4]$ to $[Cu_8]$, are also indicated in Table 7.

The above review shows the importance of metal–metal interactions in the formation, or additional stabilization, of many sulfide and sulfosalt structures containing copper. Some of them formed as ordered phases at low temperatures. The others represent low-temperature modifications of original high-temperature forms with mobile Cu atoms and stationary sulfur (± semimetal) arrays [*e.g.*, wittichenite Cu_3BiS_3 and skinnerite Cu_3SbS_3 (Makovicky *et al.* 1975, Karup-Møller & Makovicky 1974), chalcocite Cu_2S (Buerger & Wuensch 1963, Sadanaga *et al.* 1965)].

Thus the Cu–Cu interactions, averaged over space and time, might contribute to the stability of the Cu(2) spinners in tetrahedrite. The interesting questions that arise and that we plan to examine further are: (1) the potential mobility of Cu(2) in the spinner cavity at elevated (*i.e.*, mineral-formation) temperatures, and (2) the influence of possible Cu(2) ordering in the cavity on stability or symmetry (or both) of tetrahedrite at very low temperatures.

The interatomic distances between the flat pyramidal Cu(2) (at the r.m.s. distance) and Sb (at rest) are 2.98, 3.02 and 3.06 Å, respectively, for the Cu-poor, Cu-rich and substituted tetrahedrite. These contact distances lie above the values given for Cu–Sb bonds in Cu_2Sb (2.62–2.83 Å: Elander *et al.* 1935).

The S(2) position

The S(2) position of the spinners is fully occupied in the Cu-rich phase and nine-tenths occupied in the Cu-poor phase (Table 2). However, the occupancy and the temperature factor of S(2) have the largest estimated standard errors of all structure parameters and change considerably with refinement (Tables 2 and 3). Therefore, the difference in the calculated site-occupancy for S(2) in the Cu-poor phase from unity (twice the estimated standard error) cannot be considered significant.

Thus, both Cu-rich and Cu-poor tetrahedrites have the S(2) position essentially fully occupied. Our results are in agreement with the results of Wuensch (1964), Wuensch *et al.* (1966) and Kalbskopf (1972) on substituted tetrahedrite, tennantite and freibergite, respectively.

Belov & Pobedimskaya (1969) argued that S(2) is in excess, and that the Cu(2) atoms are only coordinated by two sulfur atoms and form a metal cluster $[Cu_6]$ in the spinner cavity. In their electron-diffraction study Avilov *et al.* (1971a, b) thought they had confirmed Belov's arguments. However, the accuracy of their work and their conclusions were justifiably disputed (SR 37A/1971, referee's comments). Edenharter *et al.* (1971) revised the results of Wuensch *et al.* (1966) and confirmed that the S(2) site in tennantite is fully or nearly fully occupied.

In our refinements, the *R* value dropped with the addition of S(2), by about 3% in both cases (*cf.*, Edenharter *et al.* 1971). The occupancies and the temperature factors of S(2) correlated only moderately during the entire refinement (Table 3). There is no doubt about the presence of S(2) in our phases. The compositional evidence concerning the thirteenth sulfur in the formula of tetrahedrite was discussed by Makovicky & Skinner (1978).

Pauling (1970) suggested that S(2) has transargononic, and S(1) argononic electron-configuration, contrary to Belov *et al.* (1969), who admit only argononic configuration. Several sulfur atoms coordinated by 5 and 6 copper atoms can be found in the structure of low chalcocite (Evans 1971).

The mobile-copper array

As mentioned above, the rest of the copper indicated by the chemical formulae (Makovicky & Skinner 1978) cannot be located using higher-theta X-ray reflections. The mobile portion represents about 7% of total copper in the Cu-poor phase and about 28% of total Cu in the Cu-rich phase. From all lower coordination sites along the conduction paths in the tetrahedrite structure, only the triangular planar site adjacent to the bases of the [SbS_3] pyramid of the Cu-rich phase displays a diffuse peak of electron density. It was refined as Cu(3) with the site occupancy of only 0.1 Cu, and with a very high temperature-factor (refined as a biaxial ellipsoid with $\beta_{11}=\beta_{22}=\beta_{33}=0.021(3)$ and $\beta_{12}=\beta_{31}=\beta_{23}=-0.006(2)$, equivalent isotropic $B=9.17$). The (stationary) Cu(3)–S(1) distances are 2.17 Å (2x) and 2.35 Å, average 2.23 Å; the Cu–Sb distances are 2.49 and 2.88 Å. The shorter Cu–S and Cu–Sb distances are too short. However, the oblate ellipsoids of S(1) and Sb (Table 5) show that, as a rigid body, the entire [SbS_3] pyramid of the Cu-rich phase undergoes random displacements parallel to its base (*i.e.*, perpendicular to the three-fold axis). The displacements are apparently connected with the transition of mobile copper through the Cu(3) sites and with the changes in the size of [$Cu(1)S_4$] tetrahedra when vacated by Cu(1) and on transition of mobile Cu through their faces. Proper orientations of displacements for S(1), Sb and Cu(3) (Table 5) readily yield interatomic distances consistent with stationary distances in sulfides and in Cu_2Sb (Elander *et al.* 1935).

The Cu(3) maxima suggest that the empty regions of the spinner cavity play a role as the conduction paths. The contacts Cu(3)–Cu(2) represent normal Cu–Cu contacts, whereas Cu(3) and Cu(1) are mutually exclusive (distance of 2.26 Å). No electron-density bridges between different Cu positions were observed.

An alternative interpretation of the diffuse maxima as a result of the rotation of the axis, although compatible with the distances to Sb and Cu(1), yields unacceptable 'S'–S and 'S'–Cu(2) contacts. It also contradicts the full occupancy of S(1) found in the structure refinement (Tables 2 and 3).

Thus the Cu-rich (and to some extent also Cu-poor) unsubstituted tetrahedrite represents a *room-temperature solid electrolyte* (O'Keeffe & Hyde 1976), with mobile copper ions. The reversible and immediate exsolution processes (Skinner *et al.* 1972, Tatsuka & Morimoto 1973, Makovicky & Skinner 1978), and the ready diffusion of copper (Tatsuka & Morimoto 1973), are in agreement with our structural data. The exsolution/homogenization process suggests that the mobility or the number of mobile ions (or both) visibly increase with temperature and make the entire range of tetrahedrite solid solution stable above 127.5°C. The range of the solid solution becomes more limited again at 359°C (Skinner *et al.* 1972), when a new solid electrolyte (Cu_3SbS_3: Makovicky & Skinner 1972, 1975) appears, representing a more stable phase for the compositions richer in Sb.

The stability of the tetrahedrite solid-solution

Investigations of the bearing (1) of tetrahedrite at and below the sublattice (*i.e.*, Cu–array) melting/freezing temperatures (or during the Faraday transition: O'Keeffe & Hyde 1976) and (2) of the influence of building ordered stationary arrays from the mobile Cu atoms on the symmetry or stability (or both) of unsubstituted tetrahedrite will be of great interest. Tatsuka & Morimoto (1977) suggested that on long dry annealing at 250°C the Cu-rich tetrahedrite (and presumably the entire unsubstituted tetrahedrite solid-solution) decomposes. Thus, the tetrahedrite solid-solution should only be metastable at room temperatures. However, syntheses of unsubstituted tetrahedrites from simple sulfides in aqueous ammonium chloride solution at 200°C (Lind & Makovicky, unpubl. data) still yield tetrahedrite which decomposes into the Cu-rich and Cu-poor components on quenching.

The crystal structure of Cu-poor tetrahedrite suggests possible reasons for the existence of the boundary constant-*a* parameter that separates the observed compositions of unsubstituted tetrahedrite from the ideal composition of $Cu_{12}Sb_4S_{13}$ (Makovicky & Skinner 1978). A decrease in the lattice parameter *a* is connected with a decrease in the average size of tetrahedra

[SbS_3] pyramid by 180° around the three-fold [Cu(1)S_4] and of the cavities in the tetrahedral network. The reduction of the radius of the spinner cavity is accompanied by the compression of the S(1)–S(1) (*i.e.*, peripheral) edges of the [Cu(2)S_3] triangles and the corresponding distension of the [SbS_3] pyramids. Thus, two critical interatomic distances occur: the S(1)–S(1) distance in the edge of the Cu(1) tetrahedron, perpendicular to the $\bar{4}$ axis (Wuensch *et al.* 1966), and the very short S(1)–S(1) distance in the peripheral edge of the Cu(2) triangle. Linear extrapolation of these S–S distances towards the ideal composition $Cu_{12}Sb_4S_{13}$ yields 3.65 and 3.33 Å, respectively. The former distance represents the lower limits of the common S–S distance in the Cu coordination polyhedra of the Cu sulfosalts, although still shorter unshared edges of [CuS_4] tetrahedra have been observed ($\geqq$ 3.46 Å in nowackiite: Marumo 1967). The distances comparable with the latter distance of 3.33 Å are unknown to us in the similar Cu positions. It already lies close to the minimal intermolecular S–S distances in various forms of elemental sulfur (3.20 Å: Donohue *et al.* 1961; 3.31 Å: Abrahams 1961; 3.44 Å: Watanabe 1974). It also is comparable with the *shortest* S–S distances observed in sulfosalts in various structural positions, primarily in the tight p^3 coordination pyramids of As and Sb, or in the positions in which the S–S contacts are stressed in order to achieve the best overall structural accommodation. For example, in the structure of galkhaite (Divjaković & Nowacki 1975), closely related to tetrahedrite, in which the $Cu(2)_6$ S(2) spinners are replaced by a single, statistically occurring atom of Tl and the [Cu(1)S_4] tetrahedra by large, regular tetrahedra [HgS_4], the latter short S–S contact is compressed to 3.276 Å. Alternative reasons for the low-Cu boundary were discussed by Makovicky & Skinner (1978).

The bond angles and interatomic distances (Table 4) show that in the series from Cu-rich to Cu-poor compositions, the shapes of the three principal coordination polyhedra of the structure, those of Sb, Cu(1) and Cu(2), change very little. Thus, the contraction of the stationary portion of the structure towards the Cu-poor end of the tetrahedrite solid-solution represents approximately a similarity operation (Shubnikov 1961) for all structure elements. Therefore, the existence of the solubility gap in the series at low temperatures apparently results from the stability problems of the mobile copper array at these temperatures, or from the problems involved in its interactions with the stationary atoms [primarily Cu(1)]. The chemical evidence (Makovicky & Skinner 1978) and the present refinement show that, for the low contents of Sb, only the unsubstituted tetrahedrites with ~ 10.8 Cu(1) + 12 Cu(2) + ~ 2 Cu (mobile) atoms and with 8 Cu(1) + 12 Cu(2) + ~ 8 Cu (mobile) atoms in a unit cell exist at room temperature.

ACKNOWLEDGEMENTS

We are obliged to Dr. L. Finger, Carnegie Institution, Washington D.C., for his kind assistance and for the use of his single-crystal diffractometer. The help of Mrs. M. Makovicky, Mr. F. D. Luce and Mrs. T. Kock is gratefully acknowledged. This research has been supported by the National Science Foundation, U.S.A. (grant GA–4142) and by the State Research Council, Denmark (grant 511–3594).

REFERENCES

ABRAHAMS, S. C. (1961): Scale factors, form factors, and bond lengths in orthohombic sulphur. *Acta Cryst.* 14, 311.

AHMED, R. R. (1968): *NRC-8, Fourier for Distorted and Undistorted Nets.* Div. Pure Phys., Nat. Res. Council Can., Ottawa.

AVILOV, A. S., IMAMOV, R. M. & MURADYAN, L. A. (1971a): An electron diffraction study of some phases in the Cu–Sb–S system. *Sov. Phys. – Cryst.* 15, 616-619.

———, ——— & PINSKER, Z. G. (1971b): Diffraction of 350-kV electrons by Cu_3SbS_3 crystals. *Sov. Phys. – Cryst.* 16, 533-534.

BELOV, N. V. & POBEDIMSKAYA, E. A. (1969): Covelline (klockmannite) – chalcocite (acanthite, stromeyerite, bornite) — fahlerz, *Sov. Phys. — Cryst.* 13, 843-847.

———, ZAGAL'SKAYA, YU. & POBEDIMSKAYA, E. A. (1969): Periodicheskii zakon i kristallokhimiya *In* Sto let Periodicheskogo Zakona Khimicheskikh Elementov. Nauka, Moscow.

BUERGER, M. J. & WUENSCH, B. J. (1963): Distribution of atoms in high-chalcocite, Cu_2S. *Science* 141, 276-277.

BUSING, W. R., MARTIN, K. O. & LEVY, H. A. (1962): ORFLS, a Fortran crystallographic least-squares program. *Oak Ridge Nat. Lab., TN, Rep. TM*-305.

CAMBI, L. & ELLI, M. (1965): Processi idrotermali. Sintesi di solfosali da ossidi di metalli e metalloidi. II. Cuprosolfoantimoniti. *Chim. Ind.* 47, 136-147.

Cromer, D. T. (1965): Anomalous dispersion corrections computed from self-consistent field relativistic Dirac–Slater wave functions. *Acta Cryst.* **18**, 17-23.

——— & Waber, J. T. (1965): Scattering factors computed from relativistic Dirac–Slater wave functions. *Acta Cryst.* **18**, 104-109.

Deming, W. E. (1964): *Statistical Adjustment of Data.* Dover Publ. Inc. New York.

Divjakovic, V. & Nowacki, W. (1975): Die Kristallstruktur von Galchait $[Hg_{0.76}(Cu,Zn)_{0.24}]_{12}Tl_{0.96}(AsS_3)_8$. *Z. Krist.* **142**, 262-270.

Donnay, J. D. H. & Ondik, H. M., eds. (1973): *Crystal data* (3d ed.). 2. *Inorganic Compounds* U.S. Dep. Commerce, N.B.S. & J.C.P.D.S., Washington, D.C.

Donohue, J., Aimery, C. & Goldfish, E. (1961): The crystal and molecular structure of S_6 (sulfur-6). *J. Amer. Chem. Soc.* **83**, 3748-3751.

Edenharter, A., Koto, K. & Nowacki, W. (1971): Uber Pearceit, Polybasit und Binnit. *Neues Jahrb. Mineral. Monatsh.*, 337-341.

Elander, M., Hägg, G. & Westgren, A. (1935): The crystal structure of Cu_2Sb and Fe_2As. *Ark. Kem. Mineral. Geol.* 12B(1), 1-6.

Evans, H. T., Jr. (1971): Crystal structure of low chalcocite. *Nature Phys. Sci.* **232**, 69-70.

——— & Konnert, J. A. (1976): Crystal structure refinement of covellite. *Amer. Mineral.* **61**, 996-1000.

Frueh, A. J., Jr. (1955): The crystal structure of stromeyerite, AgCuS: a possible defect structure. *Z. Krist.* **106**, 299-307.

Hall, S. R. & Rowland, J. F. (1973): The crystal structure of synthetic mooihoekite, $Cu_9Fe_9S_{16}$. *Acta Cryst.* **B29**, 2365-2372.

——— & Stewart, J. M. (1973): The crystal structure refinement of chalcopyrite, $CuFeS_2$. *Acta Cryst.* **B29**, 579-585.

Hamilton, W. C. (1959): On the isotropic temperature factor equivalent to a given anisotropic temperature factor. *Acta Cryst.* **12**, 609-610.

Hesse, R. & Aava, U. (1970): Crystal and molecular structure of the copper (I) dipropylthiocarbarmate hexamer. *Acta Chem. Scand.* **24**, 1355-1366.

Iglesias, J. E., Pachali, K. E. & Steinfink, H. (1972): The crystal structures and phase transition of α and β $BaCu_4S_3$. *Mat. Res. Bull.* **7**, 1247-1258.

Jánosi, A. (1964): La structure de sulfure cuivreux quadratique. *Acta Cryst.* **17**, 311-312.

Johnson, C. K. (1965): ORTEP, A Fortran thermal–ellipsoid plot program for crystal structure illustrations. *Oak Ridge Nat. Lab., TN.*

Kalbskopf, R. (1971): Die Koordination des Quecksilbers im Schwazit. *Tschermaks Mineral. Petrog. Mitt.* **16**, 173-175.

——— (1972): Strukturverfeinerung des Freibergits. *Tschermaks Mineral. Petrog. Mitt.* **18**, 147-155.

———, Petrlik, F. & Zemann, J. (1975): Verfeinerung der Kristallstruktur des Covellins, CuS, mit Einkristalldaten. *Tschermaks Mineral. Petrog. Mitt.* **22**, 242-249.

Karup-Møller, S. & Makovicky, E. (1974): Skinnerite, Cu_3SbS_3, a new sulfosalt from the Ilímaussaq alkaline intrusion, South Greenland. *Amer. Mineral.* **59**, 889-895.

Kocman, V. & Nuffield, E. W. (1973): The crystal structure of wittichenite, Cu_3BiS_3. *Acta Cryst.* **B29**, 2528-2535.

Koto, K. & Morimoto, N. (1970): The crystal structure of anilite. *Acta Cryst.* **B26**, 915-924.

——— & ——— (1975): Superstructure investigation of bornite, Cu_5FeS_4, by the modified partial Patterson function. *Acta Cryst.* **B31**, 2268-2273.

Kupcik, V. (1974): Antimony. Crystal chemistry. *In* Handbook of Geochemistry (K. H. Wedepohl, ed.) **II/4**, Springer-Verlag, Berlin.

——— & Makovicky, E. (1968): Die Kristallstruktur des Minerals (Pb, Ag, Bi) $Cu_4Bi_5S_{11}$. *Neues Jahrb. Mineral. Monatsh.*, 236-237.

Lawton, S. L., Rohrbaugh, W. J. & Kokotailo, G. T. (1972): The crystal and molecular structure of the tetranuclear metal cluster complex copper (I) 0, 0′ – diisopropylphosphorodithioate, $Cu_4\ [(i\text{-}C_3H_7O)_2PS_2]_4$. *Inorg. Chem.* **11**, 612-618.

Lewis, J. Jr. & Kupcik, V. (1974): The crystal structure of $Bi_2Cu_3S_4Cl$. *Acta Cryst.* **B30**, 848-852.

Machatschki, F. (1928): Formel und Kristallstruktur des Tetraedrites. *Nor. Geol. Tidsskr.* **10**, 23-32.

Makovicky, E., Makovicky, M. & Skinner, B.J. (1975): Crystallography and phase transitions of copper-rich sulphosalts between 25°C and 170°C. *Fortschr. Mineral.* **53**, (Bh. 1). 52 (Abstr.).

——— & Skinner, B. J. (1972): Crystallography of Cu_3SbS_3. *Amer. Cryst. Assoc. Winter Meet.* **61** (Abstr.).

——— & ——— (1975): On crystallography and structures of copper-rich sulphosalts between 25°–170°C. *Acta Cryst.* **A31**, S65 (Abstr.).

——— & ——— (1976): Crystal structures of synthetic tetrahedrites $Cu_{12+\delta}Sb_4S_{13}$ and $Cu_{14-\delta}Sb_4S_{13}$. *Neues Jahrb. Mineral. Monatsh.*, 141-143.

——— & ——— (1978): Studies of the sulfosalts of copper. VI. Low-temperature exsolution in synthetic tetrahedrite solid solution, $Cu_{12+x}Sb_{4+y}S_{13}$. *Can. Mineral.* **16**, 611-623.

Mariolacos, K., Kupcík, V., Ohmasa, M. & Miehe, G. (1975): The crystal structure of $Cu_4Bi_5S_{10}$ and its relation to the structures of hodrushite and cuprobismuthite. *Acta Cryst.* **B31**, 703-708.

Marumo, F. (1967): The crystal structure of nowackiite, $Cu_6Zn_3As_4S_{12}$. *Z. Krist.* **124**, 352-368.

——— & NOWACKI, W. (1964): The crystal structure of lautite and of sinnerite, a new mineral from the Lengenbach quarry. *Schweiz. Mineral. Petrog. Mitt.* **44**, 439-454.

——— & ——— (1967): A refinement of the crystal structure of luzonite, Cu_3AsS_4 *Z. Krist.* **124**, 1-8.

MATZAT, E. (1972): Die Kristallstruktur des Wittichenits, Cu_3BiS_3. *Tschermaks Mineral. Petrog. Mitt.* **18**, 312-316.

MCCANDLISH, L. E., BISSELL, E. C., COUCOUVANIS, D., FACKLER, J.P. & KNOX, K. (1968): A new metal cluster containing a cube of metal atoms. *J. Amer. Chem. Soc.* **90**, 7357-7359.

NELSON, J. B. & RILEY, D. P. (1945): An experimental investigation of extrapolation methods in the derivation of accurate unit-cell dimensions of crystals. *Phys. Soc. London Proc.* **57**, 160-177.

OHMASA, M. & MARIOLACOS, K. (1974): The crystal structure of $(Pb_{1-x},Bi_x)Bi_2Cu_2Cu_{2-x}S_5I_2(x = 0.88)$. *Acta Cryst.* B30, 2640-2643.

O'KEEFFE, M. & HYDE, B. G. (1976): The solid electrolyte transition and melting in salts. *Phil. Mag.* **33**, 219-224.

OZAWA, T. & NOWACKI, W. (1975): The crystal structure of, and the bismuth–copper distribution in synthetic cuprobismuthite. *Z. Krist.* **142**, 161-176.

PALACHE, C., BERMAN, H. & FRONDEL, C. (1951): *Dana's System of Mineralogy* 2, 7th ed. John Wiley & Sons, Inc., New York.

PAULING, L. (1970): Crystallography and chemical bonding of sulfide minerals. *Mineral Soc. Amer. Spec. Pap.* **3**, 125-131.

——— & NEUMAN, E.W. (1934): The crystal structure of binnite, $(Cu,Fe)_{12}As_4S_{13}$, and the chemical composition and structure of minerals of the tetrahedrite group. *Z. Krist.* **88**, 54-62.

RÜDORFF, W., SCHWARZ, H. G. & WALTER, M. (1952): Strukturuntersuchungen an Alkalithiocupraten. *Z. anorg. Chem.* **269**, 141-152.

SADANAGA, R., OHMASA, M. & MORIMOTO, N. (1965): On the statistical distribution of copper ions in the structure of β-chalcocite. *Mineral. J. Japan* **4**, 275-290.

SHUBNIKOV, A. V. (1961): Symmetry of similarity. *Sov. Phys. Cryst.* **5**, 469-476.

SKINNER, B. J., LUCE, F. D. & MAKOVICKY, E. (1972): Studies of the sulphosalts of copper. III. Phases and phase relations in the system Cu–Sb–S. *Econ. Geol.* **67**, 924-938.

SPARKS, R. A. (1961): Comparison of various least-squares refinement techniques. *In* Computing Methods and the Phase Problem in X-Ray Crystal Analysis (R. Pepinsky, J. M. Robertson, J. C. Speakman, eds.), Pergamon, Oxford.

SPRINGER, G. (1969): Electron probe analyses of tetrahedrite. *Neues Jahrb. Mineral. Monatsh.*, 24-32.

SZYMAŃSKI, J. T. (1974): A refinement of the structure of cubanite, $CuFe_2S_3$. *Z. Krist.* **140**, 218-239.

TAKÉUCHI, Y. (1970): On the crystal chemistry of sulphides and sulphosalts. *In Volcanism and Ore Genesis* (T. Tatsumi, ed.), Univ. Tokyo Press, Tokyo.

——— & OZAWA, T. (1975): The structure of $Cu_4Bi_4S_9$ and its relation to the structure of covellite, CuS and bismuthinite, Bi_2S_3. *Z. Krist.* **141**, 217-232.

TATSUKA, K. & MORIMOTO, N. (1973): Composition variation and polymorphism of tetrahedrite in the Cu–Sb–S system below 400°C. *Amer. Mineral.* 58, 425-434.

——— & ——— (1977): Tetrahedrite stability relations in the Cu–Sb–S system. *Econ. Geol.* **72**, 258-270.

WATANABE, Y. (1974): The crystal structure of monoclinic γ-sulphur. *Acta Cryst.* **B30**, 1396-1401.

WELLS, A. F. (1975): *Structural Inorganic Chemistry.* Clarendon, Oxford.

WUENSCH, B. J. (1964): The crystal structure of tetrahedrite, $Cu_{12}Sb_4S_{13}$. *Z. Krist.* **119**, 438-453.

——— & PREWITT, C. T. (1965): Corrections for X-ray absorption by a crystal of arbitrary shape. *Z. Krist.* **122**, 24-59.

———, TAKÉUCHI, Y. & NOWACKI, W. (1966): Refinement of the crystal structure of binnite, $Cu_{12}As_4S_{13}$. *Z. Krist.* **123**, 1-20.

Received October 1978; revised manuscript accepted January 1979.